HHS Public Access

Author manuscript

Biochim Biophys Acta Mol Cell Biol Lipids. Author manuscript; available in PMC 2020 October 01.

Published in final edited form as:

Biochim Biophys Acta Mol Cell Biol Lipids. 2019 October ; 1864(10): 1384–1395. doi:10.1016/j.bbalip.2019.06.013.

Photosystem I oligomerization affects lipid composition in *Synechocystis* sp. PCC 6803

Terezia Kovacs[1], **Balazs Szalontai**[2], **Kinga Kłodawska**[3], **Radka Vladkova**[4], **Przemysław Malec**[3], **Zoltan Gombos**[1], **Hajnalka Laczko-Dobos**[5,*]

[1]Institute of Plant Biology, Biological Research Centre, Hungarian Academy of Sciences, H-6701 Szeged, Hungary [2]Institute of Biophysics, Biological Research Centre, Hungarian Academy of Sciences, H-6701 Szeged, Hungary [3]Department of Plant Physiology and Biochemistry, Faculty of Biochemistry, Biophysics and Biotechnology, Jagiellonian University, 30-387 Kraków, Poland [4]Institute of Biophysics and Biomedical Engineering, Bulgarian Academy of Sciences, Acad. G. Bonchev Str., Bl. 21, 1113, Sofia, Bulgaria [5]Institute of Genetics, Biological Research Centre, Hungarian Academy of Sciences, H-6701 Szeged, Hungary

Abstract

In cyanobacteria, increasing growth temperature decreases lipid unsaturation and the ratio of monomer/trimer photosystem I (PSI) complexes. In the present study we applied Fourier-transform infrared (FTIR) spectroscopy and lipidomic analysis to study the effects of PSI monomer/oligomer ratio on the physical properties and lipid composition of thylakoids. To enhance the presence of monomeric PSI, a *Synechocystis* sp. PCC6803/Δ*psaL* mutant strain (*PsaL*) was used which, unlike both trimeric and monomeric PSI-containing wild type (WT) cells, contain only the monomeric form. The protein-to-lipid ratio remained unchanged in the mutant but, due to an increase in the lipid disorder in its thylakoids, the gel to liquid-crystalline phase transition temperature (Tm) is lower than in the WT. In thylakoid membranes of the mutant, digalactosyldiacylglycerol (DGDG), the most abundant bilayer-forming lipid is accumulated, whereas those in the WT contain more monogalactosyldiacylglycerol (MGDG), the only non-bilayer-forming lipid in cyanobacteria. In *PsaL* cells, the unsaturation level of sulphoquinovosyldiacylglycerol (SQDG), a regulatory anionic lipid, has increased. It seems that merely a change in the oligomerization level of a membrane protein complex (PSI), and thus the

[*]**corresponding author:** Hajnalka Laczko-Dobos, dobosh@gmail.com, Tel: +36 62 599 679, Address: Institute of Genetics, Biological Research Centre, Hungarian, Academy of Sciences, H-6701 Szeged, Hungary.

Individual contributions:
Terezia Kovacs: Investigation; Formal analysis; Methodology; Visualization; Software; Writing - original draft.
Balazs Szalontai: Investigation; Conceptualization; Writing - original draft.
Kinga Kłodawska: Data curation; Formal analysis; Writing - original draft.
Radka Vladkova: Writing - review & editing.
Przemysław Malec: Conceptualization; Writing - review & editing.
Zoltan Gombos: Conceptualization; Funding acquisition; Resources.
Hajnalka Laczko-Dobos: Conceptualization; Investigation; Formal analysis; Project administration; Supervision; Validation; Writing - original draft.

altered protein-lipid interface, can affect the lipid composition and, in addition, the whole dynamics of the membrane. Singular value decomposition (SVD) analysis has shown that in *PsaL* thylakoidal protein-lipid interactions are less stable than in the WT, and proteins start losing their native secondary structure at much milder lipid packing perturbations. Conclusions drawn from this system should be generally applicable for protein-lipid interactions in biological membranes.

Keywords

lipidomic analysis; infrared spectroscopy; PSI oligomers; *PsaL* mutant; *Synechocystis*; protein-lipid interaction

1. Introduction

Synechocystis sp. PCC6803 (hereafter *Synechocystis*) is a unicellular mesophilic cyanobacterium and a popular model organism in photosynthesis research because its photosynthetic apparatus is very similar to that of higher plants (Stanier and Cohen-Bazire, 1977). Their cell envelope is composed of an outer and a plasma membrane, separated by a peptidoglycan layer (Murata and Omata, 1988). Thylakoid membranes are the sites of oxygenic photosynthesis, they are located in the cytosol and are the most dominant membrane structures in the cell (Sakurai et al., 2006a) composed of lipids and photosynthetic protein complexes. The lipid matrix of these membranes consists of two uncharged galactolipids, constituting the majority of thylakoid membrane lipids: the non-bilayer-forming monogalactosyldiacylglycerol (MGDG) and the bilayer-forming digalactosyldiacylglycerol (DGDG). They are synthesized consecutively in the same biosynthetic pathway. Additionally, thylakoids also contain two anionic lipids, sulphoquinovosyldiacylglycerol (SQDG) and phosphatidylglycerol (PG), which are also bilayer-forming lipids (Deme et al., 2014; van Eerden et al., 2015). SQDG and PG are minor lipids of thylakoid membranes but they play indispensable roles in various cellular functions, such as cell division and photosynthesis (Aoki et al., 2012; Kobayashi et al., 2017; Kobori et al., 2018; Sato, 2004; Sato et al., 2017). As intermediate in the MGDG and DGDG biosynthetic pathway a further non-bilayer-forming lipid, monoglucosyldiacylglycerol (MGlcDG) is also present in cyanobacterial thylakoids (Awai et al., 2014; Sato and Murata, 1982; Shan et al., 2016), and it appears to be important for low-temperature survival (Yuzawa et al., 2014).

Lipid molecules can be found not only around the main photosynthetic complexes like Photosystem II (PSII) and Photosystem I (PSI), but they can also be their integral components, as has been shown by X-ray crystallography (Guskov et al., 2009; Jordan et al., 2001; Kubota et al., 2010; Loll et al., 2005; Malavath et al., 2018; Umena et al., 2011) and by lipid analysis of purified complexes (Kobayashi et al., 2017; Kubota et al., 2010; Sakurai et al., 2006b). These lipid molecules have important roles in the structure and function of photosynthetic complexes (Domonkos et al., 2008; Kobayashi, 2016; Mizusawa and Wada, 2012).

Within a lipid class, typified by specific hydrophilic headgroups, lipids can differ by acyl chain length and level of saturation. The desaturation pathway of fatty acids is well studied

in *Synechocystis* (Los and Mironov, 2015; Los and Murata, 1998; Yuzawa et al., 2014). It is known that under photoautotrophic growth conditions expression of the desaturase genes *desA, desB* and *desD* is enhanced in cells exposed to low temperature (Los et al., 1993), resulting in increased levels of membrane fatty acid desaturation (Wada and Murata, 1990). Lipid desaturation and concomitant alteration of fatty acyl chain disorder is one of the most important tool in adjusting membrane dynamics to the growth temperature (Laczko-Dobos and Szalontai, 2009; Los and Zinchenko, 2009; Murata et al., 1992; Nishida and Murata, 1996; Sinetova and Los, 2016; Szalontai et al., 2003). The expression levels of lipid desaturase genes depend not only on temperature but also on the intensity (Kis et al., 1998; Ludwig and Bryant, 2011) and spectral properties of light (Mironov et al., 2014).

In *Synechocystis* thylakoids, PSI can be present in both monomeric and trimeric forms (Boekema et al., 1987; Grotjohann and Fromme, 2005), in contrast to higher plants where only PSI monomers are present (Chitnis, 1996). In some other cyanobacteria, dimers or tetramers of PSI can be found (Li et al., 2014; Watanabe et al., 2011; Zakar et al., 2018). In *Synechocystis* a small subunit of the PSI complex, the *PsaL* protein, is required for the trimerization (Chitnis and Chitnis, 1993; Chitnis et al., 1993). The *PsaL* mutant, obtained by inactivation of the *psaL* gene (Klodawska et al., 2015) contains exclusively PSI monomers. This was the mutant that we used in the present work.

The exact role of PSI oligomers is not elucidated yet. It has been shown that several factors can influence the oligomerization state of PSI, such as growth temperature, lipid and carotenoid molecules, as well as lipid unsaturation. Recently PSI trimerization was shown to be enhanced in *Synechocystis* cells grown at elevated temperatures (Klodawska et al., 2015). It was also demonstrated that lipid unsaturation can promote PSI oligomerization (Zakar et al., 2017). In the absence of PG molecules PSI oligomers disassemble to monomers (Domonkos et al., 2004). In a total carotenoid-less mutant no PSI oligomers could be detected (Sozer et al., 2010). It was recently shown that among carotenoids xanthophylls may have an important role in stabilizing PSI oligomers (Toth et al., 2015; Zakar et al., 2017). Especially zeaxanthin and echinenone were found to be important in the fine tuning the assembly of PSI oligomers (Vajravel et al., 2017).

Here, we show that changing only the PSI trimers to monomers in cyanobacterial thylakoid membranes strongly alters the composition and unsaturation of lipids, resulting changes in physical parameters like lipid fatty acyl chain disorder and membrane dynamics. Lipid chemical changes were revealed by lipidomic analyses, whereas alterations in physical properties of the membranes by FTIR spectroscopy.

2. Materials and methods

2.1. Strains and growth conditions

Synechocystis WT and its *PsaL* mutant were grown photoautotrophically in BG11 medium (Allen, 1968) supplemented with 5 mM HEPES-NaOH (pH 7.5) under continuous white light illumination (40 μmol photons m^{-2} s^{-1}) and aeration by a gyratory shaker operating at 150 rpm. The mutant strain was grown in the presence of kanamycin and spectinomycin (both 40 μg ml^{-1}). Cultures were cultivated for three days at temperatures 25°C (below

optimum), 30°C (optimum) and 35°C (above optimum). Throughout the text samples will be referred to with symbols derived from the names of the strains and their cultivation temperatures (e.g. WT25, *PsaL*35).

2.2. Isolation of thylakoids by sucrose gradient centrifugation

Thylakoids were isolated by the method of (Murata and Omata, 1988), with some modifications. The 0.2% lysozyme-treated (37°C, 2 h) and pelleted cells were disrupted with 0.1 mm glass beads in a Bead Beater homogenizer (Biospec Products, Bartlesville, OK, USA) in the presence of 1 mM phenylmethylsulfonyl fluoride (PMSF) protease inhibitor. The disrupted cells were treated with 0.1% DNase for 15 min, and unbroken cells were removed by centrifugation (10 min, 7,000×g, 4°C). Membrane vesiculi were ultracentrifuged in a discontinuous sucrose density gradient (130,000×g, 16 h, 4°C). After flotation centrifugation thylakoids formed a green band at the interface between the 39% and 50% sucrose layers. The sucrose solution was removed and thylakoids were collected by another step of ultracentrifugation (162,000×g, 2h, 4°C). The pellet was resuspended in 10 mM TES buffer and stored at −80°C.

2.3. Fourier-transform infrared (FTIR) spectroscopy measurements

For infrared measurements, 100 μl thylakoid membrane suspension (from the −80°C stock) was diluted in 1 ml D_2O-based PBS solution in an Eppendorf tube. For complete $H_2 \rightarrow D_2O$ exchange thylakoids were collected by centrifugation (15,000×g, 7 min), re-suspended in D_2O-PBS, and then collected again by centrifugation. The pellet was layered between CaF_2 windows separated by a 15 μm thick aluminum spacer and placed in a Bruker IFS66 Fourier transform infrared spectrometer using thermostated sample holder. The temperature was increased from 12°C to 85°C in 2°C steps. The accuracy of the temperature regulation was 0.1°C. After absorption spectrum recording at a given temperature, the temperature was set to the next value and 7 min were left to reach the new temperature equilibrium. For each infrared spectrum 512 interferograms were collected (at 2 cm^{-1} spectral resolution) both for the background and sample single beam spectra (using a sample shuttle), from which the infrared absorption spectrum of the sample was calculated with the Opus software of Bruker. Frequencies of the $\nu_{sym}CH_2$ bands at around 2852-55 cm^{-1} were determined by fitting Lorentzian curves and a linear background to the spectra in the 2830-2865 cm^{-1} region. Details of the process can be found in (Kota et al., 1999). Gel to liquid-crystalline phase transition temperature was determined by fitting a Fermi function to the thermotropic response curve of the $\nu_{sym}CH_2$ frequencies. All data manipulations were performed by using the SPSERV software - © Bagyinka, Cs., BRC, Szeged, Hungary.

2.4. Singular Value Decomposition (SVD) analysis

Since in the infrared spectra there are distinct regions characteristic for lipids and proteins, studying the correlation between them upon a changing external parameter may reveal the nature and dynamics of their interactions.

For lipids we utilized the C-H stretching region between 3050-2800 cm^{-1}, having contributions mostly from the fatty-acyl chains. To follow the secondary structure changes of the proteins we used the Amide-I region between 1700-1600 cm^{-1}, which originates

mainly from the C=O stretching of the peptide bonds, thus reporting on secondary structure elements (α-helices, β-structures, etc.). For studying protein dynamics, and conditions at the protein-lipid interface, the Amide-II region (1580-1515 cm^{-1}) was utilized. When put into deuterium-based solutions, the H of the NH peptide groups become deuterated. Since the frequency of the N-D deformation band is about 100 cm^{-1} lower than the 1550 cm^{-1} frequency of the peptide N-H deformation band, this latter one gradually disappears. For the exchange D needs to penetrate into the interior of the protein, therefore the rate of this disappearance is a good measure of protein dynamics. In the case of membrane proteins, however, the H-D exchange rate depends not only on the protein dynamics but also on the accessibility of proteins through the membrane lipids, i.e. on the protein-lipid interface.

For analyzing the correlations singular value decomposition (SVD) (Henry and Hofrichter, 1992), a non-supervised multivariant method was used, which did not require any *a priori* condition on the data. For details about the use of SVD on a similar problem and object, as well as its theoretical background, see Kóta et al., (1999). When a set of infrared spectra is collected as a function of an external parameter (in our case the temperature of thylakoid membrane samples, which was changed from 12 to 85°C in 40 steps), a large data matrix (D) is generated, in which the columns are the individual IR spectra and the rows contain intensities at specific wavenumbers as a function of temperature (the external parameter). Singular value decomposition (SVD) of the D data matrix is the factorization of D into the product of three matrices $D = UWV^T$, where the columns of U and V are orthonormal and the matrix W is diagonal with positive real entries. The SVD is useful for the solution of many different problems. In our case we used one of its advantage, namely that if the effective rank (the number of the significantly non-zero eigenvalues) of the D data matrix is low, then it is useful to reduce the D matrix dimension. It will be a good approximation of the original data matrix. The rank of the D matrix can be estimated from the values of the W diagonal matrix, the values of which should be considered only until they decline close to the noise level. The actual effective rank of D depends on the given experiment, but practically never exceeds 10. Consequently, during the reduction of the D matrix in most cases less than 10 **ui** and **vi** vectors (corresponding columns of the U and V matrices) and **wii** diagonal values have to be considered in a reconstruction. We considered only the first two vectors in both matrices, namely **u1** that describes the 'average' component spectrum, and ^{u2} the largest spectral variation, which has to be combined with **u1** during the reconstruction by using the **v1** and **v2** amplitude vectors. Of these **v1** describes the intensity variation of the ‘average’ infrared spectrum, while **v2** contains the intensity values of the largest spectral variation upon the increasing measuring temperatures. Results of the SVD analysis are given in the Discussion.

2.5. Lipid isolation and lipidomics

Total lipids were extracted from intact WT and *PsaL* mutant cells according to (Welti et al., 2002) with small modifications, as described previously (Zakar et al., 2017). Mass spectrometry analysis of these total lipid extracts were performed at the Kansas Lipidomics Research Center Analytical Laboratory using tandem MS-based method (see: https://www.kstate.edu/lipid/analytical_laboratory/lipid_profiling/index.html. The percentages of normalized signal intensity/mg dry weight of lipid species are averages of three independent

biological replicates. Double bond indices of total lipids and different lipid classes were calculated according to the following equation [Σ(% of normalized signal intensity/mg dry weight of lipid species × no. of double bonds)]/100, as described in (Falcone et al., 2004).

2.6. Statistics and reproducibility

All statistical analyses were carried out using OriginPro 8 and treated statistically by a t-test at significance level of at least $p < 0.05$, defined by GraphPad program. Significance levels in figures are designated as * $p<0.05$, ** $p<0.01$, *** $p<0.005$.

3. Results

3.1. Fourier-transform infrared spectroscopy of thylakoid membranes

To reveal the structure and dynamics of the thylakoid membranes FTIR spectroscopy was used. The main advantage of this non-invasive method is that different regions of the spectrum contain bands characteristic for proteins (1700-1500 cm^{-1}) or lipids (3050-2800 cm^{-1}, and 1745-1720 cm^{-1}), thus correlating changes always show real interactions between the components.

3.1.1. Protein-to-lipid ratios of thylakoids—Figs 1A and 1B show the FTIR spectra of thylakoids purified from WT and *PsaL* cells grown at below-optimal (25°C), optimal (30°C) and above-optimal (35°C) temperatures. In the 1800-1500 cm^{-1} region of the thylakoid infrared spectra there is a band at around 1745-1720 cm^{-1} assigned to the stretching vibration of the C=O group in the ester bond between the glycerol and the fatty acyl chains in the lipid molecules (Lewis et al., 1994). The other dominant signal in the Amide I region (1700-1600 cm^{-1}) is the band at around 1650 cm^{-1}. Since the former band originates exclusively from lipids, and the latter one only from proteins, any change in their relative intensity ratio reflects a change in the protein-to-lipid ratio of the thylakoid (Szalontai et al., 2003). As seen in Fig. 1, the relative lipid-to-protein ratios are the same in WT (Fig. 1A) and *PsaL* (Fig. 1B) thylakoids, and these ratios do not change beyond the experimental error within the 25-35°C temperature range. However, looking at the component bands of the Amide I region it can be seen that while these are very similar in WT and *PsaL* at 25°C and 35°C, the lower frequency component (at around 1638-46 cm^{-1}) at 35°C is broader and thus more intense in the WT. This may indicate different structure of the PSI trimers, as compared to monomers, above the optimal temperature.

3.1.2. Thermotropic evolution of lipid fatty acyl chain disorders—To look for the consequences of having trimer/monomer PSI population in WT and exclusively monomeric PSI in the *PsaL* thylakoids the CH stretching region of their infrared spectra has been analyzed. It had been observed long time ago that the frequency of the $v_{sym}CH_2$ stretching mode is sensitive for the conformation of the fatty acyl chains, and consequently, for their packing in the lipid bilayer (Casal and Mantsch, 1984). The higher is the frequency of $v_{sym}CH_2$, the higher is the amount of the gauche segments in the lipid fatty acyl chains, that is, the higher is membrane disorder (Kota et al., 1999).

Differences between thermotropic responses of the $v_{sym}CH_2$ frequencies of thylakoids prepared from WT and *PsaL* cells grown at below-optimal, optimal, and above-optimal temperatures can reveal the consequences of their differing lipid and fatty acyl chain compositions on the membrane disorder (Fig. 2).

As seen in Fig. 2, the starting frequencies (reflecting more or less gel-phase lipids) decrease with increasing growth temperature. This means that at 12°C the less unsaturated lipids of the cells grown at 35°C are closer to the pure gel phase than the more unsaturated ones from cells grown at 25°C or 30°C. Upon increasing temperature, when the gel to liquid-crystalline phase transition is completed, there is a break-point in the thermotropic responses. Above this break-point the lipids are in liquid crystalline state, therefore further temperature-induced gauche segments cause smaller disorder increase, the slope of the curves is less steep. These phenomena can also be observed in the mutant cells (Figs 2B-D). In these panels, for comparison, the thermotropic responses of the corresponding WT thylakoid lipids at each temperature are also plotted. Comparison of the WT and *PsaL* thermotropic responses reveals an additional difference, namely, at each temperature the lipid disorder is higher and the gel to liquid-crystalline phase transition completion temperature is lower in the *PsaL* than in the WT thylakoids.

3.2. Mass spectrometry analyses of isolated lipids

To reveal the biochemical basis of the observed FTIR spectroscopic differences between the WT and *PsaL* thylakoid membranes, high throughput mass spectrometry analysis was performed on lipids isolated from *PsaL* cells containing exclusively PSI monomers and from WT cells containing a mixture of PSI trimers and monomers. For lipid analyses we used extracts of whole cells rather than thylakoids in order to avoid even minor losses of some lipid molecules during thylakoid isolation. Thylakoids make up more than 90% of all cell membranes, and because other membranes contain similar lipids the obtained lipidomic data are practically those of the thylakoid membranes (Sakurai et al., 2006b). In this lipidomic section we always compare the *PsaL* mutant lipids with those of WT.

3.2.1. Changes in the lipid class distribution—The majority of the lipids identified in the WT and *PsaL* mutant belong to the MGDG and DGDG lipid classes, whereas PG and SQDG molecules are present to a lesser extent. In the *PsaL* cells grown at the optimal temperature (30°C) we can see a considerable decrease of MGDG and concomitant increase of DGDG level (Fig. 3B). We also followed the temperature effect on lipid class distribution. In the *PsaL* cells grown at 25°C (Fig. 3A) and 35°C (Fig. 3C) we could observe decrease in the level of MGDG and increase in that of DGDG. Interestingly, at temperatures above the optimum *PsaL* cells showed a marked drop in their SQDG level, too (Fig. 3C).

In the *PsaL* cells the ratio of the non-bilayer-forming MGDG versus the most abundant bilayer-forming lipid DGDG was lower than in the WT cells at each growth temperature (25, 30, 35°C). This difference was largest at 30°C (Table 1).

3.2.2. Lipid species distribution within different lipid classes—MGDG lipid molecules from WT and *PsaL* cells showed a large variety of species. The most abundant ones were polyunsaturated species like 34:3, 34:4, 34:2 and monounsaturated ones like 34:1

(Fig. 4). At 30°C we observed less 34:3 species in *PsaL* (Fig. 4A). With higher growth temperatures the relative abundance of the 34:4 and 34:3 decreased but 34:2 increased, effects seen more intensely in *PsaL* cells. The 34:1 species also increased in both the WT and, somewhat more (see Figs 4A *vs*. 4C), the *PsaL* cells.

DGDG lipids are also rich in polyunsaturated species like 34:3, 34:4, 34:2 both in *PsaL* and WT cells (Fig. 5). In 30°C-grown *PsaL* cells we can see a decrease in the level of 34:2 species (Fig. 5A). The level of four double-bond-containing 34:4 species was significantly higher in the *PsaL* cells (Fig. 5A). In samples grown at 35°C we can observe less 34:3 species in *PsaL* (Fig. 5C). At 25°C we could not detect noticeable differences between the DGDG species distribution of *PsaL* and WT cells (Fig. 5B).

PG molecules exhibited less species variety than MGDG and DGDG. The dominant species were 34:2, 34:1, 34:3 and 32:1 (Fig. 6). In *PsaL* cells grown at 30°C we observed a major decrease of 34:1 and an increase of polyunsaturated 34:3 species levels (Fig. 6B). *PsaL* cells grown at 25°C showed less 32:1 species (Fig. 6A). Upon increasing growth temperatures the relative amount of the 34:3 decreased in both types of cells, and actually disappeared from the WT grown at 35°C.

In both strains 32:1, 32:0 and 34:3, 34:2, 34:1 were the most abundant SQDG species (Fig. 7). Surprisingly, in cells grown at 30°C there is a remarkable difference between the 32:0 and 34:2 species levels in *PsaL* and WT cells (Fig. 7B). We observed an increase in the level of 34:2 species with a parallel decrease of 32:0 species in case of *PsaL*. It is worth to note that at this temperature the three double-bond-containing 34:3 species were detected only in *PsaL* cells (Fig. 7B), though this lipid species appears in the WT at 25°C (Fig. 7A). At 25°C we observed decrease in the level of 32:1 and 32:0 species with concomitant increase of 34:2 and 34:1 species in the case of *PsaL* cells (Fig. 7A). *PsaL* cells grown at 35°C showed dramatic changes in the species distribution, like decrease in 32:0 and increase in the level of 34:2 and 34:1 species (Fig. 7C).

Taken together, these results show that the statistically significant, temperature-independent differences of *PsaL*, compared to WT, include (i) the decrease of MGDG and concomitant increase of DGDG content, and (ii) the decrease of SQDG 32:0 and PG 34:1 with concomitant increase of SQDG 34:2 and PG 34:3 contents.

3.2.3. Changes in the unsaturation level of fatty acids—To get an overview of the unsaturation level in cellular membranes we calculated the double-bond indices on the basis of lipid species percentage and total double bonds identified by lipidomics. Table 2 contains the double bond indices of total lipids and those of the different lipid classes originating from WT and PsaL cells grown at different temperatures (25°C, 30°C and 35°C). At 30°C in PsaL cells we could detect a significant increase (12%) in the unsaturation level of total lipids. As expected, changes in the growing temperature had also an effect on the unsaturation level of lipids in both WT and PsaL cells. The level of unsaturation increased at 25°C, whereas at 35°C decreased in the WT and, to a lesser extent, also in the mutant. When comparing the WT and *PsaL* cells, there are no significant differences between the double

bond indices of MGDG, DGDG and PG. By contrast, there are significant double bond index increases for SQDG in the *PsaL* cells, as compared to those of the WT.

4. Discussion

The functional importance of PSI oligomerization has not been elucidated yet. Evolutionarily oligomeric PSI forms, up to tetramers, have only been found in cyanobacteria. In all eukaryotic photosynthetic organisms PSI is present exclusively in monomeric form. In *Synechocystis*, PSI is present in monomeric/trimeric forms. Growth temperature can influence the equilibrium of these forms, shifting it toward monomers at low (20°C), and toward trimers at high (37°C) growth temperatures (Klodawska et al., 2015). PSI complexes are embedded in thylakoid membranes composed of lipids and require specific lipid environments, as revealed by crystal structures of trimeric (Malavath et al., 2018) and monomeric PSI (Netzer-El et al., 2018) from *Synechocystis* and its $PsaL^{HIS}$ mutant, respectively. The trimeric PSI crystal structure contains 51 lipids (27 PG, 16 MGDG, 7 SQDG and 1 DGDG), while monomeric PSI only 8 (4 PG, 2 MGDG and 2 SQDG) of them. However, these results of X-ray crystallography could not provide direct information on the composition and properties of thylakoidal lipid compartments that are required for maintaining PSI in trimeric or monomeric form. The knowledge of both bulk lipid phase properties of the thylakoid lipid compartments and the specific solvating ability of individual lipids are equally important (Ernst et al., 2018).

In the present work we studied the effect of the *PsaL* mutation that results in the loss of the protein subunit required for the stabilization of PSI trimers. The lack of trimerization, however, has no effect on the photoautotrophic growth and photosynthetic activity of the mutant cells (Klodawska et al., 2015).

This system, beyond the point of view of photosynthesis research, is excellent as a model for studying fundamental problems of biological membranes, such as the role of the protein-lipid interactions; the effect of the relative extent of protein-lipid interface (its tightness is a prerequisite for proper functioning of a biological membrane) on proper membrane dynamics, and on the structure of the embedded proteins.

The main difference between WT and *PsaL* thylakoids is the absence or presence of PSI trimers, therefore the mutation was expected to affect the relative amounts of lipids that are at the protein-lipid interface. In principle, a change in the extent of the protein-lipid interface could alter the protein-to-lipid ratio, as well. In our case, somewhat surprisingly, the protein-to-lipid ratio did not change either between the WT and *PsaL* cells or in response to changes in the growth temperature (Fig. 1). Earlier we found very similar constancy over different growth temperatures (Laczko-Dobos and Szalontai, 2009). These findings may indicate a possible regulatory mechanism that controls the protein-to-lipid ratio of these membranes.

In addition to the unchanged protein-to-lipid ratios, the secondary structures of the proteins were also mostly similar. Only in the thylakoids of 35°C-grown cells (WT35) was observed a significant difference at the 164x, 165x cm^{-1} regions of the Amide I band (for the interpretation of these frequencies see Fig. 1), indicating altered secondary structures. This is

in good agreement with our earlier result (Klodawska et al., 2015) showing that the structure of WT PSI trimers prepared from cells grown at 37°C was different from those of cells grown at 15°C or 25°C.

When looking at the lipid fatty acyl chain disorder as revealed by the $\nu_{sym}CH_2$ frequencies, which increase with more gauche segments per fatty acyl chain, consistent differences can be observed between the WT and *PsaL* thylakoid membranes. A higher lipid disorder (higher $\nu_{sym}CH_2$ frequencies) prevails toward lower temperatures in the *PsaL* thylakoids, as compared to those of WT (Fig. 2B-D). Such a correlation between lipid unsaturation levels and their thermotropic frequencies has already been established (Szalontai et al., 2000). In our case explanation of the differences between the thermotropic responses of the WT and *PsaL* thylakoids (Fig. 2) would require the presence of more unsaturated lipids in *PsaL*. Indeed, this has been found by the lipid analysis (see total lipid double-bond indices in Table 2).

The fact that, compared to the WT, the MGDG double-bond index did not increase in the *PsaL* mutant at any of the growth temperatures (Table 2) may indicate that MGDG molecules have direct contacts with PSI complexes at sites not masked by the oligomerization. The double bond indices did not change in DGDG, either, also indicating a possibly constant role in the PSI-lipid interaction. But an increased relative amount of DGDG in *PsaL* cells, and its essential presence in the PSI trimer (Netzer-El et al., 2018) may indicate that it is very important for interacting with a certain domain of the monomeric PSI. The non-bilayer-forming MGDG (having small headgroup) can be in greater demand at more intricate surfaces of trimeric PSI, therefore it is more abundant in WT cells. By contrast, in the case of monomeric PSI, which is more exposed to the lipid phase, membrane organization can make better use of the bilayer-forming DGDG that has higher level in *PsaL* cells. Such complementary roles of MGDG and DGDG would not considerably affect membrane dynamics since their fatty acyl chain compositions are very similar.

Along similar logic, the similar unsaturatin levels and only minor temperature-dependent double bond index differences between the WT and *PsaL* cells may also indicate that PG has a constant role in the protein-lipid interaction, most probably by interacting with specific protein surface domains that are not affected by the monomerization/trimerization of PSI.

Contrastingly, more abundant SQDG lipids exhibited large double bond index changes both upon increasing growth temperatures and between WT and *PsaL* cells (Table 2). This sensitivity may point to their prominent role in the organization of the lipid phase of the membrane.

A possible mode of action in the present case can be that reduced MGDG/DGDG ratio may cause bilayer instability and disorder in the hydrophilic bilayer region due to the twice larger headgroup of DGDG. The headgroup area/acyl chain area balance might be improved by increasing the acyl chain area of bilayer forming lipids like the anionic SQDG (e.g., decrease of 32:0 and parallel increase of 34:2 content for SQDG), which is the only lipid of which the double bond indices grew considerably between WT to *PsaL* cells. Rough estimation of such chain modification (Lee et al., 2006) could not induce hydrophobic

thickness increase. Given the lipid membrane characteristics of cyanobacterial and plant thylakoid membranes revealed by molecular dynamics simulations (van Eerden et al., 2015) the *PsaL* membrane lipid bilayer seems more similar to plant than to WT cyanobacterial lipid bilayers.

The study of the protein-lipid interactions and the possible correlations between their structural alterations was addressed by singular value decomposition (SVD), a non-supervised multivariant analyzing method. SVD analyses were performed on each set of infrared spectra recorded as a function of measuring temperature (12-85 °C) for each thylakoid sample prepared from both WT and *PsaL* cells grown at 25, 30 and 35 °C. As a typical set of results the **u1** and **u2** components of the data set of WT25 thylakoids is shown in Fig. 8.

The **u1** component represents the 'average' infrared spectrum of the analyzed region, to which, in the first approximation, the **u2** component 'the largest variation' has to be mixed to obtain back the originally measured spectra (within the neglected experimental errors). The changing 'need' for mixing **u2** to **u1** is different at each temperature, due to the involved structural changes in the sample. The **v2** amplitude vectors of the SVD analysis contain this 'need' and they are plotted along the right axis in Fig. 8 as a function of the temperature (top axis). It can be seen that the shapes of the Amide I and II **v2** vectors are similar but far from being the same, and that the lipid **v2** vector is largely different from the protein-related **v2** vectors. Therefore, an analysis of the correlation between the lipid- and the protein-related structural changes may reveal effects of the *PsaL* mutation on the protein-lipid interaction and membrane organization. In Fig. 9 all variables are plotted against the lipid structural variations, i.e. as a function of the v2 vector obtained from the SVD analysis of the C-H stretching region of the given sample.

For visualizing the dependence of the absolute lipid disorder upon the SVD-determined lipid structural changes the $\nu_{sym}CH_2$ frequencies are also plotted for each sample (left axes). These plots show that the fitted $\nu_{sym}CH_2$ frequencies, i.e. the average lipid disorder in average is higher in the *PsaL* mutant. This is in agreement with their plots versus the measuring temperature shown in Fig. 2. Intriguingly, the structure-change dependence of the $\nu_{sym}CH_2$ frequencies in the WT cells is almost linear, while it strongly deviates from linearity (it is much steeper at low measuring temperatures) in the *PsaL* samples. This may point to a certain instability in the *PsaL* membranes at low temperatures. As regards the protein-related Amide I and II **v2** vectors, in each case the Amide II **v2** amplitudes start to increase at an earlier phase of the lipid structural changes than the Amide I **v2** vectors. This is due to the fact that the disappearance of the Amide II band upon increase of the measuring temperature (shown by the **u2** component in Fig. 8C) is the result of the penetration rate-dependent H to D exchange at the NH groups. Enhanced penetration of D+ can be made possible by 'loosen' lipid environment, and this is an earlier event than the profound measuring temperature-induced protein structural change, manifested in changes in the Amide I band of the infrared spectrum.

Both Amide II and Amide I changes start at relatively lower extent of the lipid structural changes in the *PsaL* thylakoids, as compared to the WT ones. This means that the proteins

enjoy a less protective, less optimized environment in the *PsaL* mutant. It should be considered that if the protein/lipid ratio remains the same in the *PsaL* membranes as it is in the WT then the many PSI monomers require a much higher proportions of lipids for being accommodated in the protein-lipid interface. Therefore, the 'lipid fitness' can be less assured in *PsaL* than in WT membranes. The cells try to encounter this problem by changing their lipid composition and level of unsaturation but, as we saw, this compensation is not perfect.

Conclusions

We present a system allowing the study of photosynthetic membranes, a very complex environment, in which only the oligomerization potential of the PSI complex is altered. In WT *Synechocystis* this protein complex is in temperature dependent monomer/trimer equilibria, whereas in the *PsaL* mutant it occurs solely in its monomeric form. We demonstrate that the mutation-triggered monomerization of PSI complexes leads to profound alterations of the lipid composition and physical properties of thylakoid membranes. A schematic illustration of how the lack of PSI oligomerization results in the above described changes in the composition and properties of thylakoid membranes is given in Fig. 10.

The main observations concerning the physical properties of thylakoids and lipid content of WT and *PsaL* can be summarized as follows:

i. Protein-to-lipid ratios calculated from FTIR data do not indicate significant difference between WT and *PsaL* thylakoids.

ii. FTIR data of isolated thylakoid membranes revealed changes that occurred parallel with growth temperatures. With decreasing culture temperatures, the phase transition between gel and liquid-crystalline states also decreased. On the other hand, the *PsaL* mutant always showed 10-12°C lower phase transition temperatures as compared to those of the WT.

iii. Relative amounts of the two dominant lipids, the non-bilayer-forming MGDG and bilayer-forming DGDG, showed contrasting changes in WT and *PsaL* cells (MGDG decreased, DGDG increased). These lipids are synthesized consecutively in the same biosynthetic pathway, thus their amount can be regulated by a single trigger. While PSI trimers require more MGDG, in their absence the synthesis can go on toward DGDG, of which more is needed in the *PsaL* mutant.

iv. Only SQDG lipids showed a marked increase, not in their abundance, but in the level of unsaturation in the *PsaL* thylakoids. This fact may point to SQDG as a key player in the adaptation of the thylakoid lipid environment to the new conditions brought about by the increased protein-lipid interface resulting from solely monomeric PSI complexes.

v. Protein 'fitness' is considerably lower in the *PsaL* membranes. The somewhat altered lipid class composition and the more desaturated and thus less densely packed lipid fatty acyl chains of the less abundant lipid classes cannot fully compensate the perturbing effect of the elevated PSI level, which results in

increased protein surface exposed to lipids at an otherwise unchanged protein-to-lipid ratio.

Supplementary Material

Refer to Web version on PubMed Central for supplementary material.

Acknowledgement

The authors are grateful to Miklos Szekeres for critical reading and correcting the manuscript. RV is thankful to the Bulgarian and Hungarian Academies of Sciences for the visits in the BRC Institute of Plant Biology.

Funding: This work was supported by the National Research, Development and Innovation Office of Hungary NKFIH [K124922, K128575 and PD128280] and the Hungarian Governmental Grant [grant number GINOP-2.3.2-15-2016-00001]. The described lipid analyses were performed at the Kansas Lipidomics Research Center Analytical Laboratory. Instrument acquisition and lipidomics method development was supported by the National Science Foundation (EPS 0236913, MCB 1413036, MCB 0920663, DBI 0521587, DBI1228622), Technology Enterprise Corporation, K-IDeA Networks of Biomedical Research Excellence (INBRE) of the National Institute of Health (P20GM103418) and Kansas State University.

Abbreviations

DGDG	digalactosyldiacylglycerol
FTIR	Fourier-transform infrared
MGDG	monogalactosyldiacylglycerol
MGlcDG	monoglucosyldiacylglycerol
PG	phosphatidylglycerol
PsaL	*Synechocystis* sp. PCC6803/Δ*psaL* mutant
PSI	photosystem I
SQDG	sulphoquinovosyldiacylglycerol
Synechocystis	*Synechocystis* sp. PCC6803
WT	wild type

References

Allen MM 1968 Simple Conditions for Growth of Unicellular Blue-Green Algae on Plates(1, 2). J Phycol. 4, 1–4. doi:10.1111/j.1529-8817.1968.tb04667.x.

Aoki M, Tsuzuki M, and Sato N 2012 Involvement of sulfoquinovosyl diacylglycerol in DNA synthesis in Synechocystis sp. PCC 6803. BMC Res Notes. 5, 98. doi: 10.1186/1756-0500-5-98. [PubMed: 22336148]

Awai K, Ohta H, and Sato N 2014 Oxygenic photosynthesis without galactolipids. P Natl Acad Sci USA. 111, 13571–13575. doi:10.1073/pnas.1403708111.

Boekema EJ, Dekker JP, Vanheel MG, Rogner M, Saenger W, Witt I, and Witt HT 1987 Evidence for a Trimeric Organization of the Photosystem-I Complex from the Thermophilic Cyanobacterium Synechococcus Sp. Febs Letters. 217, 283–286. doi:Doi 10.1016/0014-5793(87)80679-8.

Casal HL, and Mantsch HH 1984 Polymorphic phase behaviour of phospholipid membranes studied by infrared spectroscopy. Biochim Biophys Acta. 779, 381–401. [PubMed: 6391546]

Chitnis PR 1996 Photosystem I. Plant Physiol. 111, 661–669. doi:DOI 10.1104/pp.111.3.661. [PubMed: 8754676]

Chitnis VP, and Chitnis PR 1993 PsaL subunit is required for the formation of photosystem I trimers in the cyanobacterium Synechocystis sp. PCC 6803. FEBS Lett. 336, 330–334. [PubMed: 8262256]

Chitnis VP, Xu Q, Yu L, Golbeck JH, Nakamoto H, Xie DL, and Chitnis PR 1993 Targeted inactivation of the gene psaL encoding a subunit of photosystem I of the cyanobacterium Synechocystis sp. PCC 6803. J Biol Chem. 268, 11678–11684. [PubMed: 7685019]

Deme B, Cataye C, Block MA, Marechal E, and Jouhet J 2014 Contribution of galactoglycerolipids to the 3-dimensional architecture of thylakoids. Faseb J. 28, 3373–3383. doi:10.1096/fj.13-247395. [PubMed: 24736411]

Domonkos I, Laczko-Dobos H, and Gombos Z 2008 Lipid-assisted protein-protein interactions that support photosynthetic and other cellular activities. Prog Lipid Res. 47, 422–435. doi:10.1016/j.plipres.2008.05.003. [PubMed: 18590767]

Domonkos I, Malec P, Sallai A, Kovacs L, Itoh K, Shen G, Ughy B, Bogos B, Sakurai I, Kis M, Strzalka K, Wada H, Itoh S, Farkas T, and Gombos Z 2004 Phosphatidylglycerol is essential for oligomerization of photosystem I reaction center. Plant Physiol. 134, 1471–1478. doi:10.1104/pp.103.037754. [PubMed: 15064373]

Ernst R, Ballweg S, and Levental I 2018 Cellular mechanisms of physicochemical membrane homeostasis. Curr Opin Cell Biol. 53, 44–51. doi:10.1016/j.ceb.2018.04.013. [PubMed: 29787971]

Falcone DL, Ogas JP, and Somerville CR 2004 Regulation of membrane fatty acid composition by temperature in mutants of Arabidopsis with alterations in membrane lipid composition. BMC Plant Biol. 4, 17. doi:10.1186/1471-2229-4-17. [PubMed: 15377388]

Grotjohann I, and Fromme P 2005 Structure of cyanobacterial photosystem I. Photosynth Res. 85, 51–72. doi:10.1007/s11120-005-1440-4. [PubMed: 15977059]

Guskov A, Kern J, Gabdulkhakov A, Broser M, Zouni A, and Saenger W 2009 Cyanobacterial photosystem II at 2.9-A resolution and the role of quinones, lipids, channels and chloride. Nat Struct Mol Biol. 16, 334–342. doi:10.1038/nsmb.1559. [PubMed: 19219048]

Henry ER, and Hofrichter J 1992 Singular Value Decomposition - Application to Analysis of Experimental-Data. Method Enzymol. 210, 129–192.

Jordan P, Fromme P, Witt HT, Klukas O, Saenger W, and Krauss N 2001 Three-dimensional structure of cyanobacterial photosystem I at 2.5 A resolution. Nature. 411, 909–917. doi:10.1038/35082000. [PubMed: 11418848]

Kis M, Zsiros O, Farkas T, Wada H, Nagy F, and Gombos Z 1998 Light-induced expression of fatty acid desaturase genes. Proc Natl Acad Sci U S A. 95, 4209–4214. [PubMed: 9539715]

Klodawska K, Kovacs L, Varkonyi Z, Kis M, Sozer O, Laczko-Dobos H, Kobori O, Domonkos I, Strzalka K, Gombos Z, and Malec P 2015 Elevated Growth Temperature Can Enhance Photosystem I Trimer Formation and Affects Xanthophyll Biosynthesis in Cyanobacterium Synechocystis sp PCC6803 Cells. Plant and Cell Physiology. 56, 558–571. doi:10.1093/pcp/pcu199. [PubMed: 25520404]

Kobayashi K 2016 Role of membrane glycerolipids in photosynthesis, thylakoid biogenesis and chloroplast development. J Plant Res. 129, 565–580. doi:10.1007/s10265-016-0827-y. [PubMed: 27114097]

Kobayashi K, Endo K, and Wada H 2017 Specific Distribution of Phosphatidylglycerol to Photosystem Complexes in the Thylakoid Membrane. Front Plant Sci. 8, 1991. doi:10.3389/fpls.2017.01991. [PubMed: 29209350]

Kobori TO, Uzumaki T, Kis M, Kovacs L, Domonkos I, Itoh S, Krynicka V, Kuppusamy SG, Zakar T, Dean J, Szilak L, Komenda J, Gombos Z, and Ughy B 2018 Phosphatidylglycerol is implicated in divisome formation and metabolic processes of cyanobacteria. J Plant Physiol. 223, 96–104. doi:10.1016/j.jplph.2018.02.008. [PubMed: 29558689]

Kota Z, Debreczeny M, and Szalontai B 1999 Separable contributions of ordered and disordered lipid fatty acyl chain segments to nuCH2 bands in model and biological membranes: a Fourier transform infrared spectroscopic study. Biospectroscopy. 5, 169–178. doi:10.1002/(SICI)1520-6343(1999)5:3<169::AID-BSPY6>3.0.CO;2-#. [PubMed: 10380083]

Kubota H, Sakurai I, Katayama K, Mizusawa N, Ohashi S, Kobayashi M, Zhang P, Aro EM, and Wada H 2010 Purification and characterization of photosystem I complex from Synechocystis sp. PCC 6803 by expressing histidine-tagged subunits. Biochim Biophys Acta. 1797, 98–105. doi:10.1016/j.bbabio.2009.09.001. [PubMed: 19751700]

Laczko-Dobos H, and Szalontai B 2009 Lipids, Proteins, and Their Interplay in the Dynamics of Temperature-Stressed Membranes of a Cyanobacterium, Synechocystis PCC 6803. Biochemistry. 48, 10120–10128. doi:10.1021/bi9011034. [PubMed: 19788309]

Lee AG 2006 The Membrane as a System: How Lipid Structure Affects Membrane Protein Function In: Protein-Lipid Interactions. Springer Series in Biophysics, vol. 9 Mateo CR, Gómez J, Villalaín J, González-Ros JM (eds), Springer, Berlin, Heidelberg pp. 141–175 doi: 10.1007/3-540-28435-4_6.

Lewis RN, McElhaney RN, Pohle W, and Mantsch HH 1994 Components of the carbonyl stretching band in the infrared spectra of hydrated 1,2-diacylglycerolipid bilayers: a reevaluation. Biophys J. 67, 2367–2375. doi:10.1016/S0006-3495(94)80723-4. [PubMed: 7696476]

Li M, Semchonok DA, Boekema EJ, and Bruce BD 2014 Characterization and evolution of tetrameric photosystem I from the thermophilic cyanobacterium Chroococcidiopsis sp TS-821. Plant Cell. 26, 1230–1245. doi:10.1105/tpc.113.120782. [PubMed: 24681621]

Loll B, Kern J, Saenger W, Zouni A, and Biesiadka J 2005 Towards complete cofactor arrangement in the 3.0 A resolution structure of photosystem II. Nature. 438, 1040–1044. doi:10.1038/nature04224. [PubMed: 16355230]

Los D, Horvath I, Vigh L, and Murata N 1993 The temperature-dependent expression of the desaturase gene desA in Synechocystis PCC6803. FEBS Lett. 318, 57–60. [PubMed: 8436227]

Los DA, and Mironov KS 2015 Modes of Fatty Acid desaturation in cyanobacteria: an update. Life (Basel). 5, 554–567. doi:10.3390/life5010554. [PubMed: 25809965]

Los DA, and Murata N 1998 Structure and expression of fatty acid desaturases. Biochim Biophys Acta. 1394, 3–15. [PubMed: 9767077]

Los DA, and Zinchenko VV 2009 Regulatory Role of Membrane Fluidity in Gene Expression in Advances in Photosynthesis and Respiration: Lipids in Photosynthesis, Essential and Regulatory Functions. edited by Murata H. Wada, N. pp. 329–348. Springer Dordrecht, the Netherlands.

Ludwig M, and Bryant DA 2011 Transcription Profiling of the Model Cyanobacterium Synechococcus sp. Strain PCC 7002 by Next-Gen (SOLiD) Sequencing of cDNA. Front Microbiol. 2, 41. doi: 10.3389/fmicb.2011.00041. [PubMed: 21779275]

Malavath T, Caspy I, Netzer-El SY, Klaiman D, and Nelson N 2018 Structure and function of wild-type and subunit-depleted photosystem I in Synechocystis. Biochim Biophys Acta Bioenerg. 1859, 645–654. doi:10.1016/j.bbabio.2018.02.002. [PubMed: 29414678]

Mironov KS, Sidorov RA, Kreslavski VD, Bedbenov VS, Tsydendambaev VD, and Los DA 2014 Cold-induced gene expression and omega(3) fatty acid unsaturation is controlled by red light in Synechocystis. J Photochem Photobiol B. 137, 84–88. doi:10.1016/j.jphotobiol.2014.03.001. [PubMed: 24703081]

Mizusawa N, and Wada H 2012 The role of lipids in photosystem II. Biochim Biophys Acta. 1817, 194–208. doi:10.1016/j.bbabio.2011.04.008. [PubMed: 21569758]

Murata N, and Omata T 1988 Isolation of Cyanobacterial Plasma-Membranes. Method Enzymol. 167, 245–251.

Murata N, Wada H, and Gombos Z 1992 Modes of Fatty-Acid Desaturation in Cyanobacteria. Plant and Cell Physiology. 33, 933–941.

Netzer-El SY, Caspy I, and Nelson N 2018 Crystal Structure of Photosystem I Monomer From Synechocystis PCC 6803. Front Plant Sci. 9, 1865. doi:10.3389/fpls.2018.01865. [PubMed: 30662446]

Nishida I, and Murata N 1996 CHILLING SENSITIVITY IN PLANTS AND CYANOBACTERIA: The Crucial Contribution of Membrane Lipids. Annu Rev Plant Physiol Plant Mol Biol. 47, 541–568. doi:10.1146/annurev.arplant.47.1.541. [PubMed: 15012300]

Sakurai I, Shen JR, Leng J, Ohashi S, Kobayashi M, and Wada H 2006a Lipids in oxygen-evolving photosystem II complexes of cyanobacteria and higher plants. J Biochem. 140, 201–209. doi: 10.1093/jb/mvj141. [PubMed: 16822813]

Sakurai I, Shen JR, Leng J, Ohashi S, Kobayashi M, and Wada H 2006b Lipids in oxygen-evolving photosystem II complexes of cyanobacteria and higher plants. J Biochem. 140, 201–209. doi: 10.1093/jb/mvj141. [PubMed: 16822813]

Sato N 2004 Roles of the acidic lipids sulfoquinovosyl diacylglycerol and phosphatidylglycerol in photosynthesis: their specificity and evolution. J Plant Res. 117, 495–505. doi:10.1007/s10265-004-0183-1. [PubMed: 15538651]

Sato N, Ebiya Y, Kobayashi R, Nishiyama Y, and Tsuzuki M 2017 Disturbance of cell-size determination by forced overproduction of sulfoquinovosyl diacylglycerol in the cyanobacterium Synechococcus elongatus PCC 7942. Biochem Biophys Res Commun. 487, 734–739. doi:10.1016/j.bbrc.2017.04.129. [PubMed: 28450108]

Sato N, and Murata N 1982 Lipid Biosynthesis in the Blue-Green-Alga, Anabaena-Variabilis .1. Lipid Classes. Biochimica Et Biophysica Acta. 710, 271–278.

Shan YB, Liu YQ, Yang L, Nie HG, Shen SS, Dong CX, Bai Y, Sun Q, Zhao JD, and Liu HW 2016 Lipid profiling of cyanobacteria Synechococcus sp PCC 7002 using two-dimensional liquid chromatography with quadrupole time-of-flight mass spectrometry. Journal of Separation Science. 39, 3745–3753. doi:10.1002/jssc.201600315. [PubMed: 27510466]

Sinetova MA, and Los DA 2016 New insights in cyanobacterial cold stress responses: Genes, sensors, and molecular triggers. Biochim Biophys Acta. doi:10.1016/j.bbagen.2016.07.006.

Sozer O, Komenda J, Ughy B, Domonkos I, Laczko-Dobos H, Malec P, Gombos Z, and Kis M 2010 Involvement of Carotenoids in the Synthesis and Assembly of Protein Subunits of Photosynthetic Reaction Centers of Synechocystis sp PCC 6803. Plant and Cell Physiology. 51, 823–835. doi: 10.1093/pcp/pcq031. [PubMed: 20231245]

Stanier RY, and Cohen-Bazire G 1977 Phototrophic prokaryotes: the cyanobacteria. Annu Rev Microbiol. 31, 225–274. doi:10.1146/annurev.mi.31.100177.001301. [PubMed: 410354]

Szalontai B, Kota Z, Nonaka H, and Murata N 2003 Structural consequences of genetically engineered saturation of the fatty acids of phosphatidylglycerol in tobacco thylakoid membranes. An FTIR study. Biochemistry. 42, 4292–4299. doi:10.1021/bi026894c. [PubMed: 12680783]

Szalontai B, Nishiyama Y, Gombos Z, and Murata N 2000 Membrane dynamics as seen by Fourier transform infrared spectroscopy in a cyanobacterium, Synechocystis PCC 6803 - The effects of lipid unsaturation and the protein-to-lipid ratio. Bba-Biomembranes. 1509, 409–419. doi:Doi 10.1016/S0005-2736(00)00323-0. [PubMed: 11118550]

Toth TN, Chukhutsina V, Domonkos I, Knoppova J, Komenda J, Kis M, Lenart Z, Garab G, Kovacs L, Gombos Z, and van Amerongen H 2015 Carotenoids are essential for the assembly of cyanobacterial photosynthetic complexes. Bba-Bioenergetics. 1847, 1153–1165. doi:10.1016/j.bbabio.2015.05.020. [PubMed: 26045333]

Umena Y, Kawakami K, Shen JR, and Kamiya N 2011 Crystal structure of oxygen-evolving photosystem II at a resolution of 1.9 angstrom. Nature. 473, 55–U65. doi:10.1038/nature09913. [PubMed: 21499260]

Vajravel S, Kis M, Klodawska K, Laczko-Dobos H, Malec P, Kovacs L, Gombos Z, and Toth TN 2017 Zeaxanthin and echinenone modify the structure of photosystem I trimer in Synechocystis sp. PCC 6803. Biochim Biophys Acta. 1858, 510–518. doi:10.1016/j.bbabio.2017.05.001.

van Eerden FJ, de Jong DH, de Vries AH, Wassenaar TA, and Marrink SJ 2015 Characterization of thylakoid lipid membranes from cyanobacteria and higher plants by molecular dynamics simulations. Bba-Biomembranes. 1848, 1319–1330. doi:10.1016/j.bbamem.2015.02.025. [PubMed: 25749153]

Wada H, and Murata N 1990 Temperature-Induced Changes in the Fatty Acid Composition of the Cyanobacterium, Synechocystis PCC6803. Plant Physiol. 92, 1062–1069. [PubMed: 16667371]

Watanabe M, Kubota H, Wada H, Narikawa R, and Ikeuchi M 2011 Novel supercomplex organization of photosystem I in Anabaena and Cyanophora paradoxa. Plant Cell Physiol. 52, 162–168. doi: 10.1093/pcp/pcq183. [PubMed: 21118826]

Welti R, Li WQ, Li MY, Sang YM, Biesiada H, Zhou HE, Rajashekar CB, Williams TD, and Wang XM 2002 Profiling membrane lipids in plant stress responses - Role of phospholipase D alpha in freezing-induced lipid changes in Arabidopsis. J Biol Chem. 277, 31994–32002. doi:10.1074/jbc.M205375200. [PubMed: 12077151]

Yuzawa Y, Shimojima M, Sato R, Mizusawa N, Ikeda K, Suzuki M, Iwai M, Hori K, Wada H, Masuda S, and Ohta H 2014 Cyanobacterial monogalactosyldiacylglycerol-synthesis pathway is involved in normal unsaturation of galactolipids and low-temperature adaptation of Synechocystis sp PCC 6803. Bba-Mol Cell Biol L. 1841, 475–483. doi:10.1016/j.bbalip.2013.12.007.

Zakar T, Herman E, Vajravel S, Kovacs L, Knoppova J, Komenda J, Domonkos I, Kis M, Gombos Z, and Laczko-Dobos H 2017 Lipid and carotenoid cooperation-driven adaptation to light and temperature stress in Synechocystis sp. PCC6803. Biochim Biophys Acta. 1858, 337–350. doi: 10.1016/j.bbabio.2017.02.002.

Zakar T, Kovacs L, Vajravel S, Herman E, Kis M, Laczko-Dobos H, and Gombos Z 2018 Determination of PS I oligomerisation in various cyanobacterial strains and mutants by non-invasive methods. Photosynthetica. 56, 294–299. doi:10.1007/s11099-018-0795-7.

Highlights:

- Protein-lipid interactions are decisive in determining the structure of membranes
- PSI oligomerization affects physical properties and lipid composition of thylakoids
- PSI monomer-containing thylakoids show increased lipid disorder
- Monomer PSI favors DGDG-, whereas its trimeric form MGDG-rich membrane environment
- Increased unsaturation level of the anionic lipid SQDG supports PSI monomers

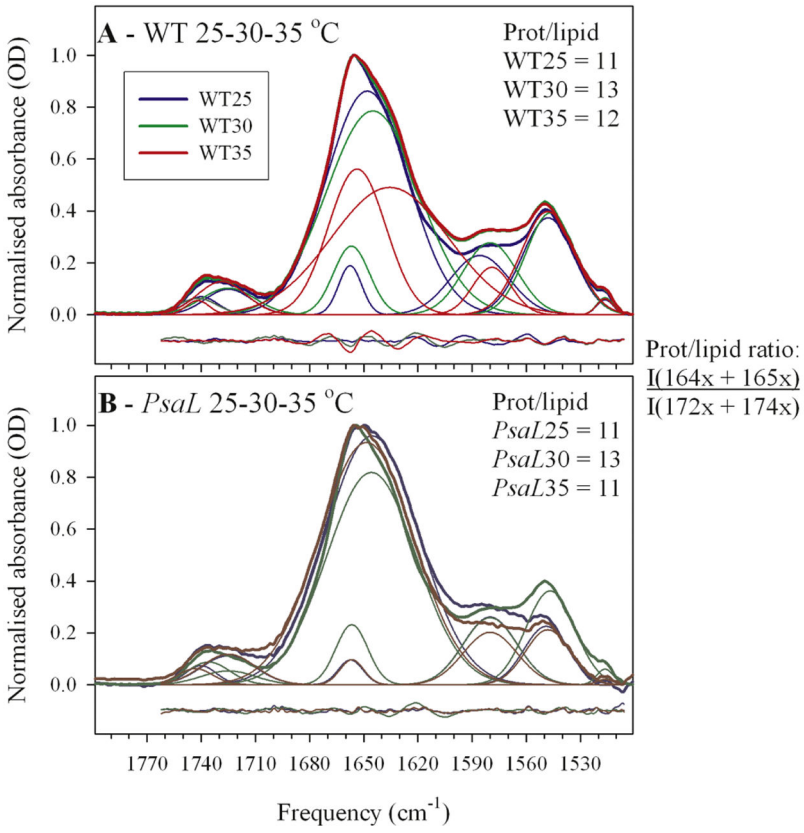

Figure 1.

Infrared spectra of wild type (WT) and *PsaL* mutant (*PsaL*) thylakoids prepared from cells grown at 25, 30 and 35 °C. Protein-to-lipid ratios were obtained by dividing the summed integrals of the protein-related 164x, 165x cm^{-1} of the Amide I band with the summed integrals of the lipid ester C=O band components (at 172x and 174x cm'^{1}). The x indicates that in the individual free fits of the spectra there was a variation in the last digit of the obtained component bands at around 1636-48 cm^{-1}, 1654-58 cm^{-1}, and 1725 cm^{-1}, 1740-45 cm^{-1}, respectively. Note that the protein-to-lipid ratios remained practically unchanged independently of mutation and of growth temperature (in agreement with earlier results of Laczko-Dobos and Szalontai, 2009)

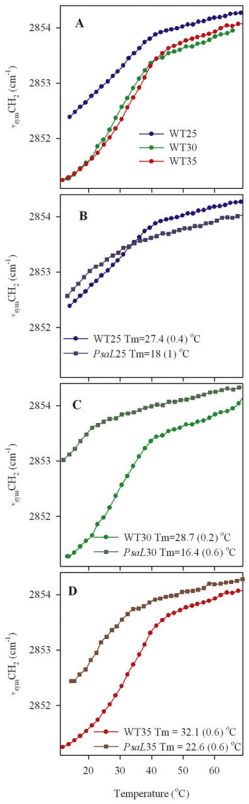

Figure 2.

Thermotropic responses of the $v_{sym}CH_2$ frequencies in *Synechocystis* WT (Panel A) and *PsaL* mutant thylakoids, compared to responses of the WT grown at 25, 30 and 35°C. (Panels B-D). Tm: middle temperature of the gel-to-liquid crystalline phase transition. Errors of the Tm determinations are given in parentheses.

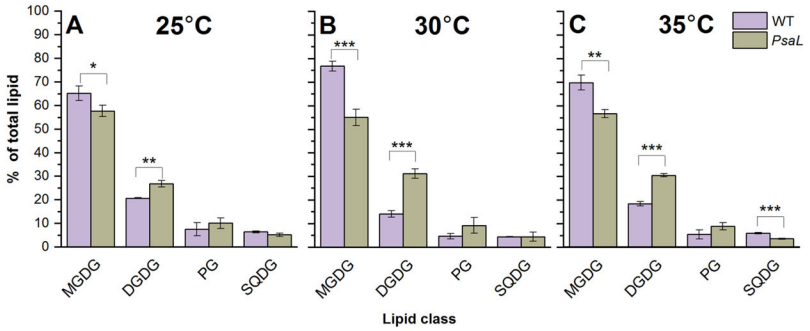

Figure 3.

Lipid-class distribution of wild-type (WT) cells and *PsaL* mutant (*PsaL*) grown at 25°C (panel A), 30°C (panel B) and 35°C (panel C). The most abundant lipid classes are: MGDG (monogalactosyldiacylglycerol) and DGDG (digalactosyldiacylglycerol). The minor lipids are: PG (phosphatidylglycerol) and SQDG (sulphoquinovosyldiacylglycerol). Significance levels in figures are designated as * $p<0.05$, ** $p<0.01$, *** $p<0.005$.

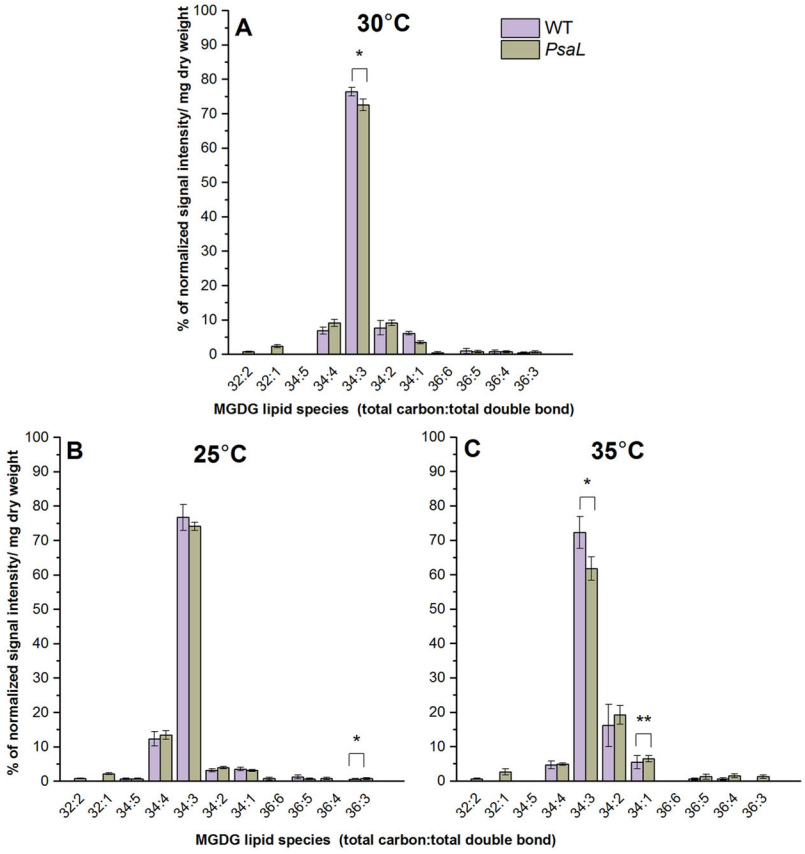

Figure 4.

Percentages of the most abundant lipid species belonging to the MGDG class from WT and *PsaL* cells grown at 30°C (panel A), 25°C (panel B) and 35°C (panel C). Lipid species are denoted as total carbon number:total double bond. Significance levels in figures are designated as * $p<0.05$, ** $p<0.01$, *** $p<0.005$.

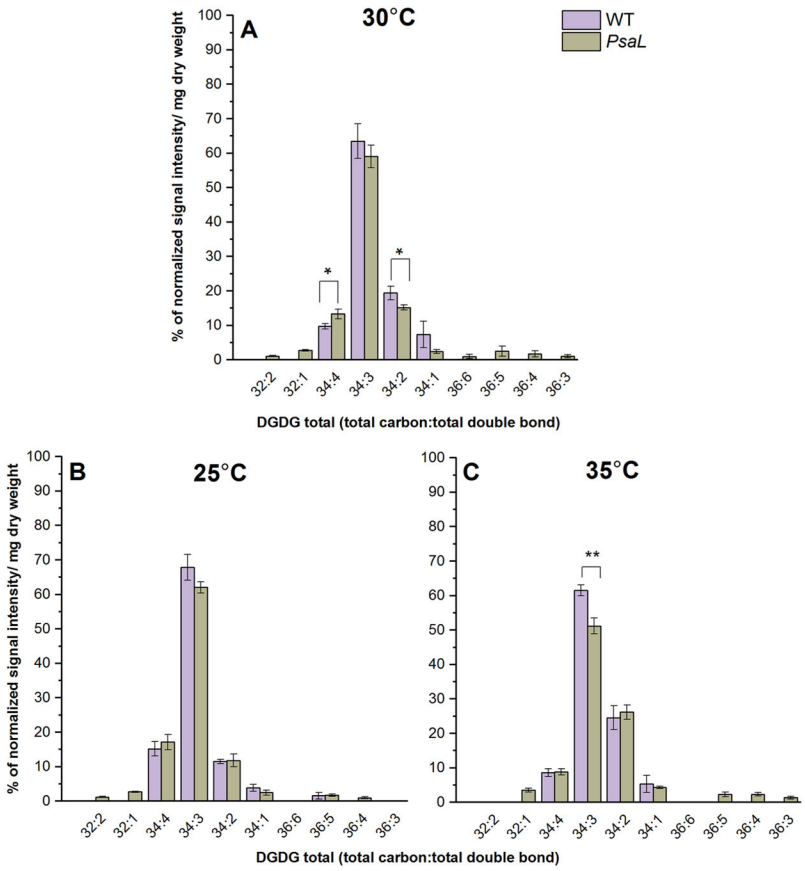

Figure 5.

Percentages of the most abundant lipid species belonging to the DGDG class from WT and *PsaL* cells grown at 30°C (panel A), 25°C (panel B) and 35°C (panel C). Lipid species are denoted as total carbon number:total double bond. Significance levels in figures are designated as * $p<0.05$, ** $p<0.01$, *** $p<0.005$.

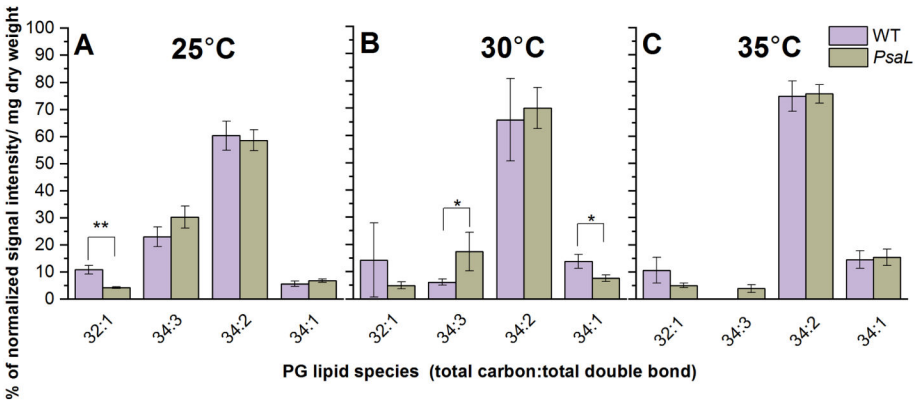

Figure 6.

Percentages of the most abundant lipid species belonging to the PG class from WT and PsaL cells grown at 25°C (panel A), 30°C (panel B) and 35°C (panel C). Lipid species are denoted as total carbon number:total double-bond. Significance levels in figures are designated as * $p<0.05$, ** $p<0.01$, *** $p<0.005$.

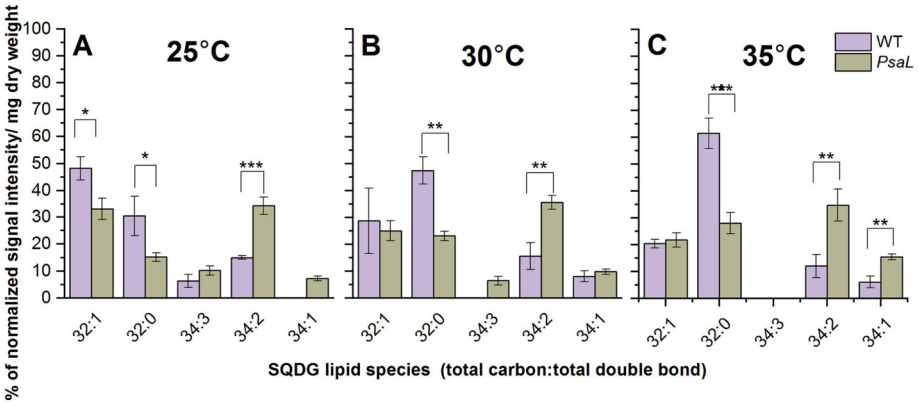

Figure 7.

Percentages of the most abundant lipid species belonging to the SQDG class from WT and *PsaL* cells grown at 25°C (panel A), 30°C (panel B) and 35°C (panel C). Lipid species are denoted as total carbon number:total double bond. Significance levels in figures are designated as * $p<0.05$, ** $p<0.01$, *** $p<0.005$.

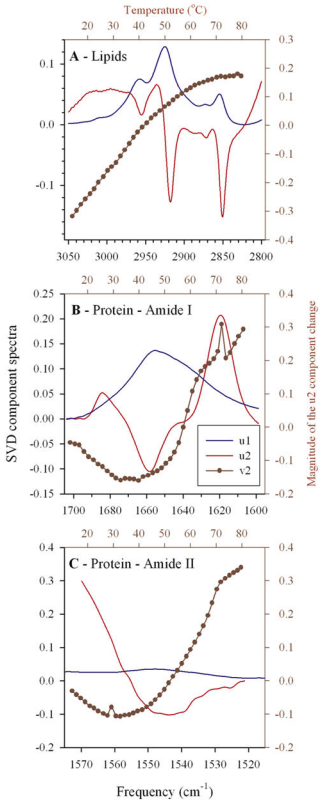

Figure 8.

Typical examples (from WT25thylakoids) for the result of the multivariant Singular Value Decomposition (SVD) analysis of **u1** (the 'average') in **blue**, the **u2** (the 'largest change') in **red**, and the amplitudes (**v2** vectors) of the **u2** components in dark red for the CH stretching. The analyzed regions of the infrared spectra were: Lipids – (3050-2800 cm^{-1}), Amide I – (1700-1600 cm^{-1}), and Amide II – (1575-1515 cm^{-1}). Bottom and left axes correspond to **u1** and **u2** spectra, top and right axes to the **v2** amplitudes. For details, see the text.

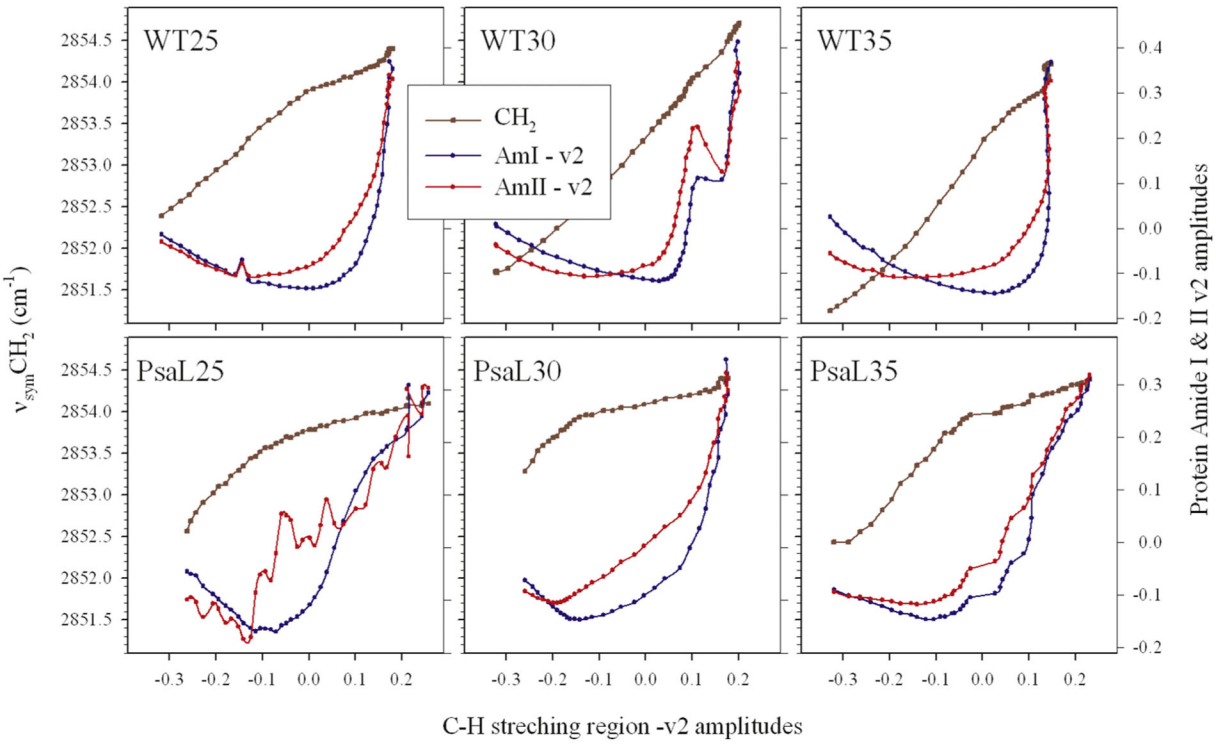

Figure 9.

Absolute fatty acyl chain disorders and protein ⇔ lipid structural change correlations in thylakoid membranes of WT and *PsaL* grown at 25, 30 and 35 °C. The left axes correspond to the $\nu_{sym}CH_2$ frequencies obtained by fitting a Lorentzian-shaped curve to each measured spectrum around the $\nu_{sym}CH_2$ band (2830-2860 cm^{-1}); the right axes show the amplitudes of the Amide I and II **v2** vectors (the amplitudes of the largest spectral changes) as a function of the largest lipid structural change (the **v2** vectors of the C-H stretching region). The amplitude vectors were obtained from the SVD of sets of temperature dependent measurement of infrared spectra performed on thylakoid membranes. Samples are indicated as WT25,30,35 and *PsaL*25, 30, 35, respectively.

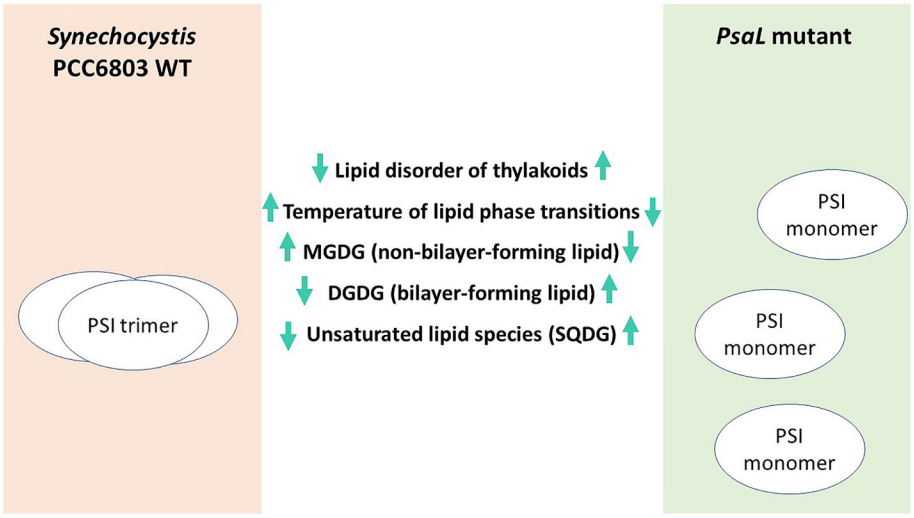

Figure 10.

Lipid-protein interactions and their effect on the physical properties and lipid composition of thylakoids in wild-type (WT) *Synechocystis* and its only PSI monomer-containing *PsaL* mutant. Mentioned lipid classes are: MGDG (monogalactosyldiacylglycerol), DGDG (digalactosyldiacylglycerol), SQDG (sulphoquinovosyldiacylglycerol).Up and down arrows indicate the directions of changes observed in the *PsaL* mutants compared to WT.

Table 1.

MGDG/DGDG lipid ratios of WT and *PsaL* cells grown at 25°C, 30°C and 35°C.

	Cyanobacterial strains, MGDG/DGDG lipid ratio ± SD	
Temperature (°C)	**WT**	***PsaL***
25	3,1±0,2	2.2±0,2
30	5,5±0,7	1,8±0,2
35	3,8±0,4	1,9±0,1

±SD values were calculated from three independent biological replicates.

Table 2.

Double-bond indices of total lipids, as well as lipid classes, from WT and *PsaL* cells grown at 25°C, 30°C and 35°C.

Lipid class	Temperature (°C)	Total double bond index of lipid species in cyanobacterial strains	
		WT	***PsaL***
MGDG	25	3,09	3,02
	30	2,91	2,90
	35	2,79	2,71
DGDG	25	2,99	2,98
	30	2,76	2,96
	35	2,73	2,74
SQDG	25	0,97	1,40
	30	**0,68**	**1,21**
	35	0,51	1,07
PG	25	2,06	2,19
	30	**1,78**	**2,01**
	35	1,75	1,83
Total lipid	25	9,12	9,58
	30	**8,13**	**9,09**
	35	7,78	8,35

Double-bond indices were calculated as described in the Materials and Methods. Main differences are highlighted in bold.